Buoy Measurements of Wind–Wave Relations during Hurricane Matthew in 2016

S. A. HSU

School of Marine Sciences, Nanjing University of Information Science and Technology, Nanjing, China, and Coastal Studies Institute, and Department of Oceanography and Coastal Sciences, Louisiana State University, Baton Rouge, Louisiana

YIJUN HE

School of Marine Sciences, Nanjing University of Information Science and Technology, Nanjing, China

HUI SHEN

School of Marine Sciences, Nanjing University of Information Science and Technology, Nanjing, China, and Bedford Institute of Oceanography, Dartmouth, Nova Scotia, Canada

(Manuscript received 19 December 2016, in final form 28 July 2017)

ABSTRACT

Studies suggested that neutral-stability wind speed at 10 m $U_{10} \geq 9$ m s^{-1} and wave steepness $H_s/L_p \geq 0.020$ can be taken as criteria for aerodynamically rough ocean surface and the onset of a wind sea, respectively; here, H_s is the significant wave height, and L_p is the peak wavelength. Based on these criteria, it is found that, for the growing wind seas when the wave steepness increases with time during Hurricane Matthew in 2016 before the arrival of its center, the dimensionless significant wave height and peak period is approximately linearly related, resulting in $U_{10} = 35H_s/T_p$; here, T_p is the dominant or peak wave period. This proposed wind–wave relation for aerodynamically rough flow over the wind seas is further verified under Hurricane Ivan and North Sea storm conditions. However, after the passage of Matthew's center, when the wave steepness was nearly steady, a power-law relation between the dimensionless wave height and its period prevailed with its exponent equal to 1.86 and a very high correlation coefficient of 0.97.

1. Introduction

Wind–wave interaction has been investigated extensively; for example, since JONSWAP by Hasselmann et al. (1973), there has been Hasselmann et al. (1976), Kahma (1981), Zakharov and Zaslavsky (1983), Donelan et al. (1985), Young (1988), Dobson et al. (1989), Wen et al. (1989), Ewans and Kibblewhite (1990), Babanin and Soloviev (1998), Young (1998), Hara and Belcher (2002), Hwang and Wang (2004), Drennan et al. (2005), Hwang (2005), Young (2006), Caulliez et al. (2008), Romero and Melville (2010), Sullivan and McWilliams (2010), Hwang et al. (2011), Holthuijsen et al. (2012), Hwang et al. (2012), Reichl et al. (2014), Hara and Sullivan (2015), Buckley and Veron (2016), Hwang (2016), and Hwang and Walsh (2016).

From 2 to 4 October 2016, Hurricane Matthew (see www.nhc.noaa.gov) passed over the National Data Buoy Center buoy 42058 located in the central Caribbean Sea (see www.ndbc.noaa.gov). Simultaneous measurements of the wind speed at 5 m U_5, significant wave height H_s, dominant wave period T_p, and other parameters were made by the NDBC (see www.ndbc.noaa.gov) as provided in Table 1. Note that prior to the arrival of Matthew's center, the wind speed increased from approximately 16 to 33 m s^{-1} (see Fig. 1), H_s increased from 4 to 10 m, and the barometric pressure dropped from 1002 to 958 hPa. This period of growing wind seas was followed by the passage of Matthew's center, which lasted about 3 h, and then the wind seas were in the decaying stage. Therefore, Table 1 provides us unique opportunity to investigate the relations between wind and wave before and after the passing of a tropical cyclone as measured by a data buoy.

2. Atmospheric stability conditions

To study the wind–wave relation, atmospheric stability conditions need to be investigated first. According to

Corresponding author: S. A. Hsu, sahsu@lsu.edu

DOI: 10.1175/JPO-D-16-0280.1

TABLE 1. Pertinent datasets as measured at NDBC buoy 42058 during the passage of Hurricane Matthew in October 2016 used in this study (data source: www.ndbc.noaa.gov).

Date	Hour (UTC)	Wind direction (deg)	U_5 (m s^{-1})	H_s (m)	T_p (s)	Wave direction (deg)	Pressure (hPa)	Air temperature (°C)	Sea temperature (°C)
2	2	55	12.2	4.08	10	102	1005.4	28.7	28.8
2	3	60	14.1	3.86	10	84	1004.7	28.7	28.8
2	4	55	12.4	4.05	10	99	1004	27.6	28.8
2	5	56	12	3.94	10	96	1003.5	28.6	28.8
2	6	68	16.1	4.16	10.81	95	1002	27.9	28.7
2	7	59	16.6	4.64	10	87	1001.2	27.6	28.6
2	8	60	15.9	5.7	10	96	1001	27.6	28.6
2	9	58	16.8	5.51	11.43	111	1001.2	27.7	28.7
2	10	66	18.2	6.14	11.43	105	1001.4	27.1	28.8
2	11	60	18	6.82	11.43	108	1001.1	27.1	28.7
2	12	53	18	7.22	10.81	103	1001.3	26.3	28.7
2	13	63	21	6.09	10.81	97	1000.9	25.5	28.7
2	14	56	20.5	7.07	11.43	110	1000.4	26.2	28.7
2	15	55	19.3	6.74	10.81	100	999.4	25.8	28.7
2	16	56	19.8	6.23	10	108	998.1	25.2	28.7
2	17	52	21.9	6.77	10	108	995.6	25.6	28.7
2	18	54	22.5	7.23	10	91	993.9	25.4	28.5
2	19	50	23.7	8.4	10	63	992.1	25	28.5
2	20	60	24.2	7.98	10.81	44	991	25.2	28.2
2	21	53	24.3	7.9	10	59	989.5	25.3	28.2
2	22	75	23.2	7.32	10	78	990.2	25.7	28.1
2	23	79	22.6	6.97	10	63	990.1	25.6	28
3	0	74	24	6.22	9.09	83	989.6	25.5	28
3	1	60	26.1	7.18	9.09	91	987.2	25.5	27.9
3	2	66	27.8	7.71	10	56	983.5	25.6	27.8
3	3	63	31.6	10.09	10	305	972.6	25.4	27.7
3	4	73	33	10.35	10.81	355	958.1	25.7	27.5
3	5	77	18.1	8.43	9.09	75	945.2	26.2	27.3
3	6, eye	264	5.6	5.8	10	110	943.7	26.3	26.9
3	7	249	28.4	4.57	10	117	946.4	26.1	26.5
3	8	243	33.2	6.58	9.09	122	959.2	25.3	26
3	9	247	27.9	6.26	10	141	973.1	25.8	25.8
3	10	246	25.5	5.58	8.33	198	978.4	26.1	25.7
3	11	240	22.3	5.52	10	341	983.7	25.9	25.7
3	12	240	21	5.03	9.09	316	986.9	26	25.6
3	13	242	19.5	4.76	9.09	316	989.6	26.1	25.7
3	14	241	21	4.97	8.33	267	991	26	25.7
3	15	235	20.4	5.23	8.33	314	991.7	26.2	25.7
3	16	237	19.2	5.17	9.09	325	993.4	26.7	25.7
3	17	236	18.2	5.93	8.33	284	994.5	26.5	25.7
3	18	225	18	5.28	8.33	266	995.9	25.6	25.7
3	19	232	16.1	5.3	8.33	215	997	26.4	25.7
3	20	231	16	5.47	9.09	325	997.8	26.9	25.7
3	21	230	14.6	4.81	8.33	302	998.7	26.5	25.6
3	22	223	15.1	4.66	9.09	330	999.8	25.8	25.6
3	23	242	14.3	4.31	8.33	224	1000.9	26.8	25.6
4	0	242	13.3	4.61	7.69	254	1002.1	26.8	25.7
4	1	238	11.8	4.34	7.69	240	1003.8	27.3	25.7
4	2	233	13	4.44	8.33	291	1003.7	27.3	25.8
4	3	244	12.1	4.1	7.69	263	1004.7	27.1	25.8
4	4	234	10.4	4.03	7.69	285	1005	27.1	25.9

Hasse and Weber (1985), overwater stability categories may be estimated using a graphic approach from the measurements of wind speed and air and sea temperature difference. By adopting their method, with data presented in Table 1, stability D prevailed during the entire period, indicating that the stability is near neutral so that the logarithmic wind profile law is valid (see Hsu 2003).

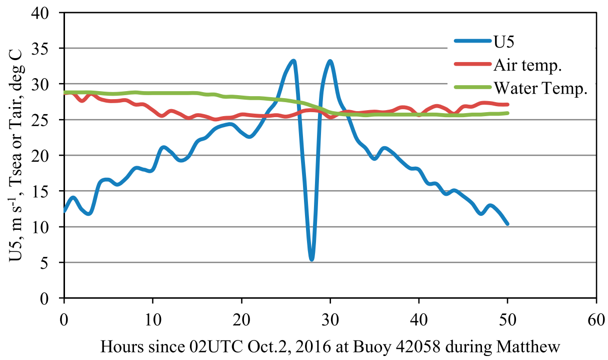

FIG. 1. Time series of U_5 (blue), water (green), and air (red) temperatures at buoy 42058 during Matthew in 2016 (data source: Table 1).

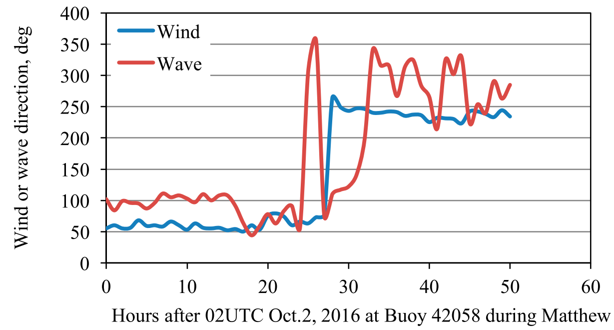

FIG. 2. Time series of wind (blue) and wave direction (red) at buoy 42058 during Matthew in 2016 (data source: Table 1).

3. Criterion for the wind sea

To minimize the effects of swell, conditions under the wind sea are investigated next. According to Drennan et al. (2005), a wind sea is defined when

$$H_s/L_p \geq 0.020, \quad \text{and} \tag{1}$$

$$L_p = (g/2\pi)T_p^2 = 1.56T_p^2. \tag{2}$$

Here, H_s is the significant wave height (m), L_p is the dominant wavelength (m), T_p is the peak or dominant wave period (s), and g is the gravitational acceleration (9.8 m s^{-2}). Note that the dimensionless parameter H_s/L_p is called wave steepness, which is available from routine buoy measurements as provided in Table 1. Using Eq. (1), all the datasets listed in Table 1 are valid under the wind-sea conditions.

4. Criterion for rough flow over the ocean

According to Andreas et al. (2012), for aerodynamically rough flow over the ocean, approximately,

$$U_{10} \geq 9\,\mathrm{m\,s^{-1}}. \tag{3}$$

Here, U_{10} is the neutral-stability wind speed at a reference height of 10 m. Since the datasets presented in Table 1 are for $U_5 \geq 9$ m s^{-1}, they were also under the condition of aerodynamically rough flow over the ocean.

5. Adjusting the wind speed from 5 to 10 m

In the atmospheric boundary layer, under near-neutral-stability conditions, the logarithmic wind profile is valid, particularly during a hurricane, as demonstrated by Hsu (2003) and Vickery et al. (2009):

$$U_z = (U_*/k)\ln(Z/Z_o). \tag{4}$$

Here, U_* is the friction velocity, k (=0.4) is the von Kármán constant, Z is the height, and Z_o is the roughness length.

According to Taylor and Yelland (2001),

$$Z_o/H_s = 1200(H_s/L_p)^{4.5}. \tag{5}$$

Because the wind speeds were recorded at 5 m instead of 10 m at buoy 42058 during Matthew in 2016, one needs to adjust U_5 to U_{10} using the logarithmic wind profile law under neutral-stability conditions (see, e.g., Hsu 2003) so that, by substituting $Z = 5$ and 10 into Eq. (4) and eliminating the term of (U_*/k), we have

$$U_{10} = U_5\ln(10/Z_o)/\ln(5/Z_o). \tag{6}$$

Now, using Eqs. (2), (5), and (6) and U_5, U_{10} can be computed.

6. Wind and wave relation during growing wind seas

From Fig. 1 and Table 1, the period for growing waves was from 0200 UTC on 2 October through 0400 UTC on 3 October. During this period, Fig. 2 indicates that both wind and wave directions were from the east. Their difference was within 60 degrees until the effects of the storm center set in.

Analytically, the dimensionless wave height gH_s/U_{10}^2 and wave period gT_p/U_{10}, are often related according to a power law (see, e.g., Hasselmann et al. 1976; Kahma 1981; Zakharov and Zaslavsky 1983; Donelan et al. 1985; Dobson et al. 1989; Wen et al. 1989; Ewans and Kibblewhite 1990; Babanin and Soloviev 1998) so that

$$gH_s/U_{10}^2 = a(gT_p/U_{10})^b. \tag{7}$$

Here, coefficients a and b need to be determined from experiments. Examples from the literature are listed as follows:

From Babanin and Soloviev (1998),

$$gH_s/U_{10}^2 = 0.01152(gT_p/U_{10})^{1.505}.$$

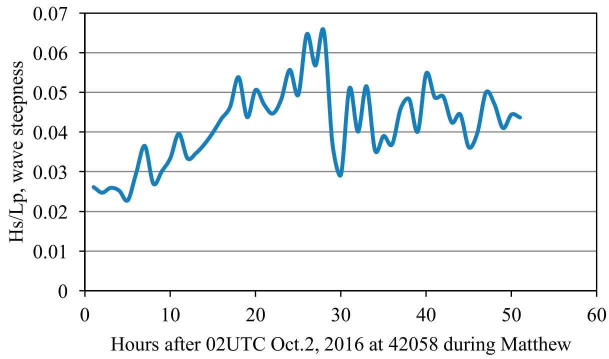

FIG. 3. Time series of wave steepness at buoy 42058 during Matthew (data source: Table 1).

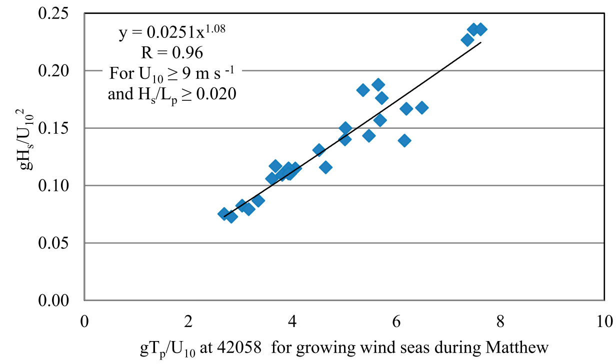

FIG. 4. Power-law relation with $b = 1.08$ in Eq. (7) for the growing wind seas during Matthew.

From Hasselmann et al. (1976),

$$gH_s/U_{10}^2 = 0.00903(gT_p/U_{10})^{1.667}.$$

From Davidan (1980),

$$gH_s/U_{10}^2 = 0.01046(gT_p/U_{10})^{1.47}.$$

From Kahma (1981),

$$gH_s/U_{10}^2 = 0.01362(gT_p/U_{10})^{1.50}.$$

From Donelan et al. (1985),

$$gH_s/U_{10}^2 = 0.00958(gT_p/U_{10})^{1.65}.$$

From Dobson et al. (1989),

$$gH_s/U_{10}^2 = 0.00897(gT_p/U_{10})^{1.65}.$$

From Wen et al. (1989),

$$gH_s/U_{10}^2 = 0.01109(gT_p/U_{10})^{1.515}.$$

From Ewans and Kibblewhite (1990),

$$gH_s/U_{10}^2 = 0.00998(gT_p/U_{10})^{1.455}.$$

From Zakharov and Zaslavsky (1983),

$$gH_s/U_{10}^2 = 0.01339(gT_p/U_{10})^{1.335}.$$

The aforementioned formulas from the literature indicate the generic power-law relation between dimensionless significant wave height, and the peak wave period does exist as provided in Eq. (7), although the coefficient a and its exponent b may vary. The datasets listed in Table 1 are unique in that both growing wind sea prior to the passage of Matthew and steady seas after its passage (see Fig. 3) are available to compare with those formulas as provided above. Now, using the computed U_{10} and measured H_s and T_p from Table 1, Fig. 4 shows that the exponent b is approximately unity, indicating that the dimensionless wave height and its period may be linearly related. Therefore, if we set $b = 1$ in Eq. (7) and using the same datasets as employed for Fig. 4, Fig. 5 shows that

$$U_{10} = 35H_s/T_p, \tag{8}$$

with a correlation coefficient $R = 0.95$.

To further verify Eqs. (7) and (8), pertinent datasets during Hurricane Ivan at buoy 42003 in 2004 are employed. (For the track and dataset of Ivan, see www.nhc.noaa.gov and www.ndbc.noaa.gov, respectively.) The period that satisfied both Eqs. (1) and (3) was from 0800 UTC 13 September to 1100 UTC 16 September 2004. Note that buoy 42003 was located on the right side of Ivan's track. The results are presented in Figs. 6 and 7, respectively. If one accepts that $R = 0.87$ in Fig. 6, Eq. (7) is verified, and that the slope = 0.94 and $R = 0.94$, Eq. (8) is validated. It is interesting to see whether Eq. (8) is also useful under extratropical cyclone conditions. This is accomplished by employing the datasets provided in Geernaert et al. (1987) as measured in the North Sea (note that T_p is not given but computed from the wave phase speed). Figure 8 shows the result. Again, if one accepts the statistics as indicated in the figure, Eq. (8) is reasonable.

7. Wind and wave relation during the steady wind seas

After the passage of Matthew's storm center (see Fig. 1), the wind seas were nearly steady (see Fig. 3). Analysis of U_{10} and measured H_s and T_p from Table 1 shows (see Fig. 9) that Eq. (7) is applicable such that

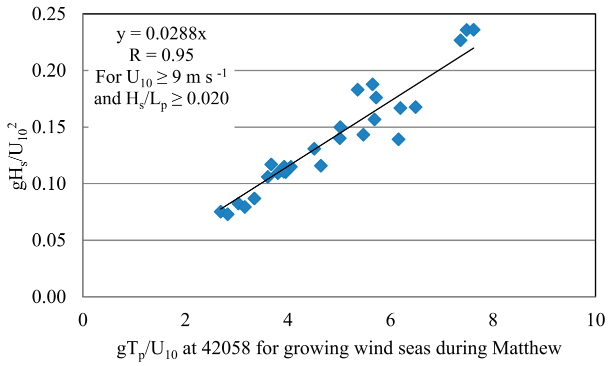

FIG. 5. Simplified linear relation by setting $b = 1$ in Eq. (7) for the growing wind seas during Matthew.

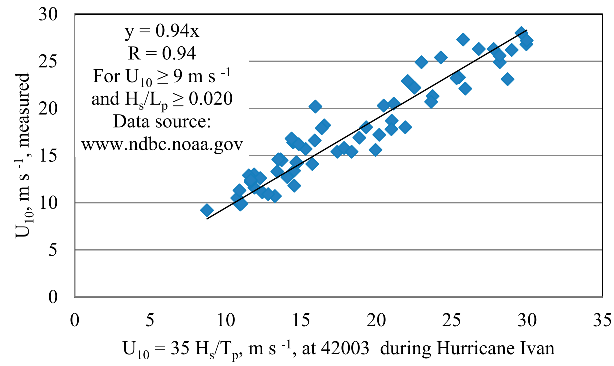

FIG. 7. Verification of Eq. (8) at buoy 42003 located on the right side of Hurricane Ivan's track.

$$gH_s/U_{10}^2 = 0.0087(gT_p/U_{10})^{1.86}, \quad (9)$$

with a very high correlation coefficient, $R = 0.97$. Note that Eq. (9) is in reasonable agreement with that of the JONSWAP formula as provided by Hasselmann et al. (1973, 1976), indicating that the wave steepness during JONSWAP experiment was nearly steady.

8. Conclusions

On the basis of the aforementioned analyses and discussions, it is concluded that, during Hurricane Matthew in 2016, when both neutral-stability wind speed at 10 m U_{10} and wave steepness exceed 9 m s^{-1} and 0.020, respectively, the dimensionless wave height and its corresponding period are related according to the power law, as indicated in the literature. However, it is also found that, during the growing wind seas, they are approximately linearly related, resulting in $U_{10} = 35H_s/T_p$. On the other hand, after the passage of Matthew's center, when the wind seas were nearly steady, the power-law relation prevailed with its exponent equal to 1.86 and correlation coefficient equal to 0.97. The proposed linear relation between dimensionless wave height and period is further verified by the measurements from a data buoy located on the right side of the track of Hurricane Ivan and extratropical cyclones over the North Sea.

The power-law functions between the dimensionless energy (wave height) and wave period implies, in a manner, a universality of wind-wave growth (Zakharov et al. 2015). However, the coefficients and exponents of such parameterizations vary in a relatively wide range in the literature, as shown in Table 2 in Badulin et al. (2007) and the examples cited in this paper. The discrepancy among models from different experiments may be due to associated different wave dynamics during the experiment and thus are not to be generalized into other situations. For example, the well-known exponents of 5/3 (Hasselmann et al. 1976), 3/2 (Toba 1972), and 4/3 (Zakharov and Zaslavsky 1983) correspond to different reference regimes of wind-wave coupling associated with permanent fluxes of momentum, energy, and wave action [see Gagnaire-Renou et al. (2011) for details]. The results presented here shed additional light

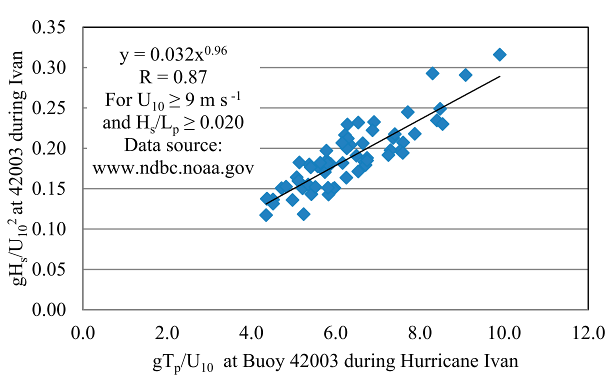

FIG. 6. Power-law relation with $b = 0.96$ in Eq. (7) during wind seas induced by Ivan at buoy 42003.

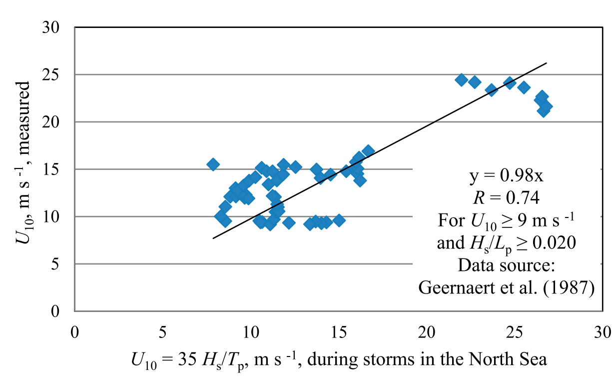

FIG. 8. Verification of Eq. (8) during extratropical cyclones over the North Sea using the datasets provided in Geernaert et al. (1987).

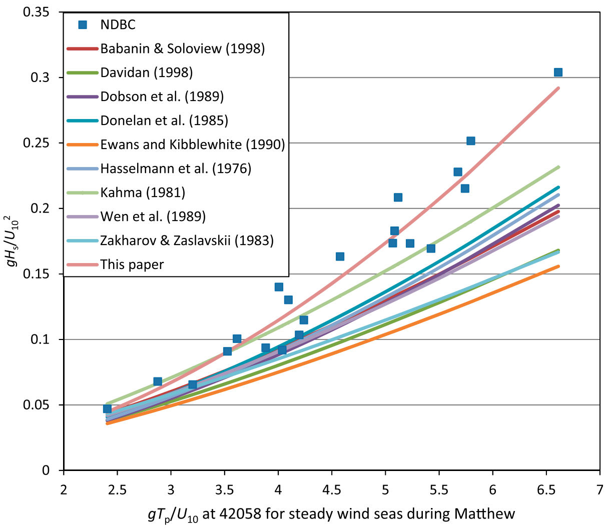

FIG. 9. Power-law relation with $b = 1.86$ in Eq. (7) for the steady wind seas during Matthew; also overlaid are models from Babanin and Soloviev (1998), Hasselmann et al. (1976), Kahma (1981), Donelan et al. (1985), Dobson et al. (1989), Wen et al. (1989), Ewans and Kibblewhite (1990), and Zakharov and Zaslavskii (1983).

on the dynamics of wind-wave development under different stages of hurricanes.

Acknowledgments. This research was supported in part by the Chinese National Program on Global Change and Air-Sea Interaction (GASI–IPOVAI-04).

REFERENCES

Andreas, E. L, L. Mahrt, and D. Vickers, 2012: A new drag relation for aerodynamically rough flow over the ocean. *J. Atmos. Sci.*, **69**, 2520–2537, doi:10.1175/JAS-D-11-0312.1.

Babanin, A. V., and Y. P. Soloviev, 1998: Field investigation of transformation of the wind wave frequency spectrum with fetch and the stage of development. *J. Phys. Oceanogr.*, **28**, 563–576, doi:10.1175/1520-0485(1998)028<0563:FIOTOT>2.0.CO;2.

Badulin, S. I., A. V. Babanin, V. E. Zakharov, and D. Resio, 2007: Weakly turbulent laws of wind-wave growth. *J. Fluid Mech.*, **591**, 339–378, doi:10.1017/S0022112007008282.

Buckley, M. P., and F. Veron, 2016: Structure of the airflow above surface waves. *J. Phys. Oceanogr.*, **46**, 1377–1397, doi:10.1175/JPO-D-15-0135.1.

Caulliez, G., V. Makin, and V. Kudryavtsev, 2008: Drag of the water surface at very short fetches: Observations and modeling. *J. Phys. Oceanogr.*, **38**, 2038–2055, doi:10.1175/2008JPO3893.1.

Davidan, I. N., 1980: Investigation of wave probability structure on field data (in Russian). *Tr. Gos. Okeanogr. Inst.*, **151**, 8–26.

Dobson, F., W. Perrie, and B. Toulany, 1989: On the deep-water fetch law for wind-generated gravity waves. *Atmos.–Ocean*, **27**, 210–236, doi:10.1080/07055900.1989.9649334.

Donelan, M. A., J. Hamilton, and W. H. Hui, 1985: Directional spectra of wind-generated waves. *Philos. Trans. Roy. Soc. London*, **A315**, 509–562, doi:10.1098/rsta.1985.0054.

Drennan, W. M., P. K. Taylor, and M. J. Yelland, 2005: Parameterizing the sea surface roughness. *J. Phys. Oceanogr.*, **35**, 835–848, doi:10.1175/JPO2704.1.

Ewans, K. C., and A. C. Kibblewhite, 1990: An examination of fetch-limited wave growth off the west coast of New Zealand by a comparison with the JONSWAP results. *J. Phys. Oceanogr.*, **20**, 1278–1296, doi:10.1175/1520-0485(1990)020<1278:AEOFLW>2.0.CO;2.

Gagnaire-Renou, E., M. Benoit, and S. I. Badulin, 2011: On weakly turbulent scaling of wind sea in simulations of fetch-limited growth. *J. Fluid Mech.*, **669**, 178–213, doi:10.1017/S0022112010004921.

Geernaert, G. L., S. E. Larsen, and F. Hansen, 1987: Measurements of the wind stress, heat flux, and turbulence intensity during storm conditions over the North Sea. *J. Geophys. Res.*, **92**, 13 127–13 139, doi:10.1029/JC092iC12p13127.

Hara, T., and S. E. Belcher, 2002: Wind forcing in the equilibrium range of wind-wave spectra. *J. Fluid Mech.*, **470**, 223–245, doi:10.1017/S0022112002001945.

——, and P. P. Sullivan, 2015: Wave boundary layer turbulence over surface waves in a strongly forced condition. *J. Phys. Oceanogr.*, **45**, 868–883, doi:10.1175/JPO-D-14-0116.1.

Hasse, L., and H. Weber, 1985: On the conversion of Pasquill categories for use over sea. *Bound.-Layer Meteor.*, **31**, 177–185, doi:10.1007/BF00121176.

Hasselmann, K., and Coauthors, 1973: Measurements of wind-wave growth and swell decay during the Joint North Sea Wave Project (JONSWAP). Ergänzungsheft zur Deutschen Hydrographischen Zeitschrift Reihe A(8) 12, 95 pp.

——, W. Sell, D. B. Ross, and P. Müller, 1976: A parametric wave prediction model. *J. Phys. Oceanogr.*, **6**, 200–228, doi:10.1175/1520-0485(1976)006<0200:APWPM>2.0.CO;2.

Holthuijsen, L. H., M. D. Powell, and J. D. Pietrzak, 2012: Wind and waves in extreme hurricanes. *J. Geophys. Res.*, **117**, C09003, doi:10.1029/2012JC007983.

Hsu, S. A., 2003: Estimating overwater friction velocity and exponent of power-law wind profile from gust factor during storms. *J. Waterw. Port Coastal Ocean Eng.*, **129**, 174–177, doi:10.1061/(ASCE)0733-950X(2003)129:4(174).

Hwang, P. A., 2005: Drag coefficient, dynamic roughness and reference wind speed. *J. Oceanogr.*, **61**, 399–413, doi:10.1007/s10872-005-0050-2.

——, 2016: Fetch- and duration-limited nature of surface wave growth inside tropical cyclones: With applications to air–sea exchange and remote sensing. *J. Phys. Oceanogr.*, **46**, 41–56, doi:10.1175/JPO-D-15-0173.1.

——, and D. W. Wang, 2004: Field measurements of duration-limited growth of wind-generated ocean surface waves at young stage of development. *J. Phys. Oceanogr.*, **34**, 2316–2326, doi:10.1175/1520-0485(2004)034<2316:FMODGO>2.0.CO;2.

——, and E. J. Walsh, 2016: Azimuthal and radial variation of wind-generated surface waves inside tropical cyclones. *J. Phys. Oceanogr.*, **46**, 2605–2621, doi:10.1175/JPO-D-16-0051.1.

——, H. Garcia-Nava, and F. J. Ocampo-Torres, 2011: Observations of wind wave development in mixed seas and unsteady wind forcing. *J. Phys. Oceanogr.*, **41**, 2343–2362, doi:10.1175/JPO-D-11-044.1.

——, F. J. Ocampo-Torres, and H. García-Nava, 2012: Wind sea and swell separation of 1D wave spectrum by a spectrum integration method. *J. Atmos. Oceanic Technol.*, **29**, 116–128, doi:10.1175/JTECH-D-11-00075.1.

Kahma, K. K., 1981: A study of growth of the wave spectrum with fetch. *J. Phys. Oceanogr.*, **11**, 1503–1515, doi:10.1175/1520-0485(1981)011<1503:ASOTGO>2.0.CO;2.

Reichl, B. G., T. Hara, and I. Ginis, 2014: Sea state dependence of the wind stress over the ocean under hurricane winds. *J. Geophys. Res. Oceans*, **119**, 30–51, doi:10.1002/2013JC009289.

Romero, L., and W. K. Melville, 2010: Airborne observations of fetch-limited waves in the Gulf of Tehuantepec. *J. Phys. Oceanogr.*, **40**, 441–465, doi:10.1175/2009JPO4127.1.

Sullivan, P. P., and J. C. McWilliams, 2010: Dynamics of winds and currents coupled to surface waves. *Annu. Rev. Fluid Mech.*, **42**, 19–42, doi:10.1146/annurev-fluid-121108-145541.

Taylor, P. T., and M. Yelland, 2001: The dependence of sea roughness on the height and steepness of the waves. *J. Phys. Oceanogr.*, **31**, 572–590, doi:10.1175/1520-0485(2001)031<0572:TDOSSR>2.0.CO;2.

Toba, Y., 1972: Local balance in the air–sea boundary processes. Part I. On the growth process of wind waves. *J. Oceanogr. Soc. Japan*, **28**, 109–121, doi:10.1007/BF02109772.

Vickery, P. J., D. Wadhera, M. D. Powell, and Y. Chen, 2009: A hurricane boundary layer and wind field model for use in engineering applications. *J. Appl. Meteor. Climatol.*, **48**, 381–405, doi:10.1175/2008JAMC1841.1.

Wen, S. C., D. C. Zhang, P. Z. Guo, and B. H. Chen, 1989: Parameters in wind-wave frequency spectra and their bearings on spectrum forms and growth. *Acta Oceanol. Sin.*, **8**, 15–39.

Young, I. R., 1988: Parametric hurricane wave prediction model. *J. Waterw. Port Coastal Ocean Eng.*, **114**, 637–652, doi:10.1061/(ASCE)0733-950X(1988)114:5(637).

——, 1998: Observations of the spectra of hurricane generated waves. *Ocean Eng.*, **25**, 261–276, doi:10.1016/S0029-8018(97)00011-5.

——, 2006: Directional spectra of hurricane wind waves. *J. Geophys. Res.*, **111**, C08020, doi:10.1029/2006JC003540.

Zakharov, V. E., and M. M. Zaslavsky, 1983: The dependence of wave parameters on wind velocity, its duration and fetch in a weak turbulence theory of wind waves. *Izv. Akad. Nauk SSSR Fiz. Atmos. Okeana*, **19**, 406–415.

——, S. I. Badulin, P. A. Hwang, and G. Caulliez, 2015: Universality of sea wave growth and its physical roots. *J. Fluid Mech.*, **780**, 503–535, doi:10.1017/jfm.2015.468.